1

Adhesion Phenomena Pertaining to Thermal Interface Materials and Solder Interconnects in Microelectronic Packaging: A Critical Review

Dinesh P R Thanu[1]*, Aravindha Antoniswamy[2], Roozbeh Danaei[3] and Manish Keswani[4]

[1]*Department of Materials Science and Engineering, University of Arizona, Tucson, AZ 85721, USA*

[2]*Department of Materials Science and Engineering, University of Texas at Austin, TX 78712, USA*

[3]*School of Mechanical and Materials Engineering, Washington State University, Pullman, WA 99163, USA*

[4]*Department of Materials Science and Engineering, University of Arizona, Tucson, AZ 85721, USA*

Abstract

High performance and diverse power computing needs in desktop, server, communication, automotive, and artificial intelligence microelectronic sectors demand microprocessors with different form factors and intricate package designs. For such complex package architectures, semiconductor chips in addition to microprocessor, such as in-package memory, transceivers or a combination of both are essential to attain maximum performance. Integrated Heat Spreader (IHS) assembly with thermal interface material (TIM) layers plays a vital role in providing heat dissipation for these integrated circuit chips and aids them to perform with maximum efficiency for a long duration. Additionally, for Ball Grid Array (BGA) semiconductor packages, interfacial adhesion quality of solder attach material is very critical in determining package quality and reliability. There are numerous challenges associated with developing and optimizing such an IHS assembly process and solder attach material for high volume manufacturing with good throughput, quality and yield. Here we provide a comprehensive review of the adhesion mechanisms and challenges of polymer TIMs to IHS-metal interface and various techniques proposed in the literature to enhance their adhesion. Complexities involved in solder attach adhesion including material selection and chip assembly interaction are reviewed in detail as well.

**Corresponding author*: dineshprt@gmail.com

K.L. Mittal (ed.) Progress in Adhesion and Adhesives, Volume 4 (1–24) © 2019 Scrivener Publishing LLC

Keywords: Adhesion, ball grid array, integrated heat spreader, interconnect, microelectronic packaging, solder flux, thermal interface material

1.1 Introduction

Integrated Heat Spreader (IHS) assembly is an integral part of a microelectronic package to accomplish efficient thermal dissipation from one or more semiconductor chips and to attain overall device thermal performance [1–5]. State-of-the-art IHS assembly process is used in various application sectors including desktop, server, communication, automotive, and artificial intelligence. In an assembly process, semiconductor chips or dies are first placed on an organic or ceramic substrate. Front layer interconnect and an underfill layer are further used to hold the dies mechanically. Furthermore, an IHS is glued on the substrate to protect the die and aid with its heat dissipation [6–8]. During IHS assembly, a thermal interface material (TIM) is placed or dispensed on the surface of the die and an adhesive or sealant material is further applied and cured on the organic substrate layer (motherboard) to mechanically hold the IHS in place. A TIM layer is placed between the die and the IHS referred to as TIM_1 and between IHS and heat sink referred to as TIM_2 as shown in Figure 1. A Ball Grid Array or BGA package is a form of surface mount technology (SMT) that is being used increasingly for integrated circuits. It has become one of the most popular packaging alternatives for high input/output devices in the industry. Apart from the improvement in connectivity they offer, BGAs have other advantages. They offer a much lower thermal resistance between the silicon chips than the quad flat pack devices. This allows heat generated by the integrated circuit inside the package to be conducted out of the device on the PCB faster and more effectively. The whole bottom surface of the device can be used on a BGA as compared to just the perimeter on a Land Grid Array (LGA)

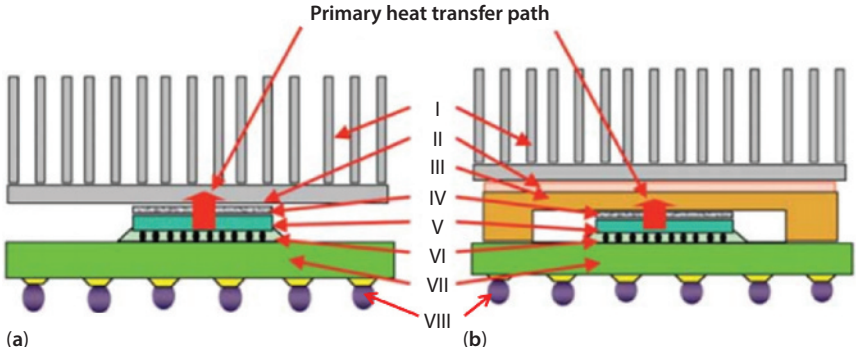

Figure 1.1 Schematics of multiple thermal architectures. (**a**) Designs typically used in laptops without an IHS (**b**) Architectures used in desktop, server and high-end gaming applications with an IHS. I- Heat Sink; II-TIM_2; III- IHS; IV- TIM_1; V- Silicon Die; VI- Underfill; VII- Substrate; VIII- Solder Ball [Adapted from [8]].

package. BGA packages have solder balls pre-attached to the bottom of the substrate, hence resulting in a higher stand-off height compared to LGA packages.

Thermal efficiency and reliability of TIM_1, TIM_2 and solder balls define the performance of a microelectronic package and its long-lasting characteristics depend a lot on the interfacial adhesion between the layers [9]. In this review, focus will be mainly on the adhesion characteristics of these materials due to their quintessential role in the microelectronic packaging. This review will be divided into two sections excluding the Introduction. Section 2 provides an overview of the thermal interface material and its interfacial adhesion phenomena. Section 3 on the other hand is devoted to the solder joint adhesion characteristic and its dependence on the material quality and assembly process.

1.2 Polymer Thermal Interface Material -Metal Interface Adhesion Phenomena

1.2.1 Basics of Thermal Interface Material Adhesion

Shown in Figure 2 is a simple graphical representation of a microelectronic package resistance network. The key temperatures of interest include T_j or T_{jmax} which refers to the maximum junction temperature in the device, T_c which refers to the IHS temperature, T_{sink} which refers to the heat sink temperature, and T_a which refers to the local ambient air temperature. Total thermal resistance which depends on the interfacial adhesion can be described as two components: junction to IHS surface resistance or package thermal resistance and heat sink surface to ambient resistance or system thermal resistance. The maximum allowable junction temperature is one of the key factors that limits the power dissipation capability of a device. The maximum power that a device can dissipate, also referred to as thermal design power (TDP), can be written as

$$TDP = (T_{jmax} - T_a)/\Psi_{ja} \tag{1}$$

$$TDP = (T_{jmax} - T_a)/(\Psi_{jc} + \Psi_{ca}) \tag{2}$$

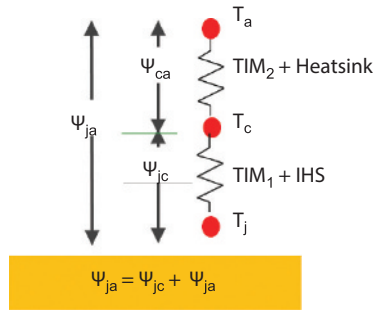

Figure 1.2 Classical example of a one-dimensional resistance network [Adapted from [10]].

$$\Psi_{jc} + \Psi_{ca} = (T_{jmax} - T_a)/TDP \quad (3)$$

In other words, TDP is the maximum amount of heat that a processor can generate for a thermally significant period while running real applications. Ψ_{ja} is the overall thermal resistance, Ψ_{jc} is the package thermal resistance and Ψ_{ca} is the system thermal resistance.

If we consider only the package level thermal resistance, equation (3) can be re-written as,

$$\Psi_{jc} = (T_{jmax} - T_c)/TDP \quad (4)$$

Thermal impedance in a package is represented universally in industry as R_{jc} and is measured as package thermal resistance (Ψ_{jc}) under uniform power times the area of the silicon die (A_{die}) as shown in equation (5).

$$R_{jc} = (\Psi_{jc})_{\text{uniform power}} \times A_{die} \quad (5)$$

Poor adhesion of the TIM layer has a huge impact on the junction temperature, increasing R_{jc} and, therefore, impacts TDP leading to poor power capability of a microelectronic device.

Real TIMs in a semiconductor package look like as shown in Figure 3. Real TIMs have a finite bondline thickness (BLT) and at the interface have voids/delamination because of their inability to completely wet the surface. From Figure 3 it can be inferred that the total thermal impedance (R_{TIM}) of a real TIM can be written as

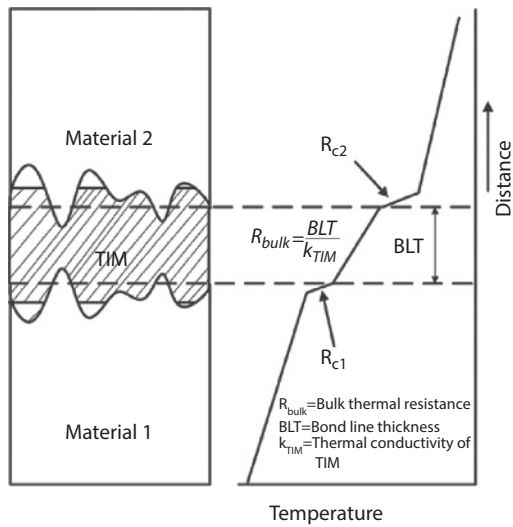

Figure 1.3 Cross-sectional illustration of a TIM layer [Adapted from [8]].

$$R_{TIM} = (BLT/ k_{TIM}) + R_{c1} + R_{c2} \quad (6)$$

where R_{c1} and R_{c2} represent the contact resistances of the TIM at the silicon-TIM and TIM-metal interfaces, respectively. There is a great drive in the semiconductor industry to decrease the R_{TIM} as much as possible to provide efficient thermal dissipation on high-end packages. One way to do this is by increasing the thermal conductivity of the TIM (k_{TIM}) using novel materials and process optimization; however, it will be of no use if the TIM fails to adhere to the surface initially or the adhesion bond weakens over a period of time. Both these failures lead to quality issues either during manufacturing impacting yield and productivity or in the field during use condition affecting product users. Customer returns because of these types of quality issues are becoming a norm these days and hence understanding the fundamentals of adhesion bonds and the root cause of adhesion failures is very critical.

1.2.2 Current Status of Thermal Interface Materials and their Bonding Mechanisms

With the recent developments in TIMs, a Polymer Thermal Interface Material (PTIM) is preferred over a Solder Thermal Interface Material (STIM) due to its inherent cost benefits and comparable thermal performance to STIM [11, 12]. IHS attachment process, in particular, can be performed in two stages: room temperature assembly and high temperature curing. Room temperature assembly is, however, not sufficient enough to bond the PTIM/STIM and sealant with IHS as these materials are not cured. Both sealant and PTIM/STIM need to be cured at high temperature (~150 °C to 180 °C) with pressure on top of these to achieve their targeted material properties and BLT. Polymer to IHS bonding is caused by a combination of different adhesion mechanisms such as physical adsorption, mechanical interlocking, and chemical bonding [13–17]. Physical adsorption forces are a resultant of interatomic and intermolecular interactions due to the van der Waals bonds. On the other hand, mechanical interlocking is brought about by surface roughness of the substrate; however it is debatable whether enhancement in adhesion strength is due to mechanical interlocking or increase in the effective area through secondary bonding [18]. Primary chemical bonds are one order of magnitude stronger than secondary chemical forces such as van der Waals force (Table 1). The primary bond type also includes acid-base theory of adhesion which is very popular and has been studied extensively on various surfaces including polymers [19–21]. By increasing the number of bonds across the interface, polymer-IHS metal bonding could be enhanced considerably.

Chemists tend to associate adhesion with the energy liberated when two surfaces meet to form an intimate contact characterized as an interface as shown in Figure 4. In other words, adhesion may be defined as the energy required to dismantle the interface between two materials. Physicists and engineers describe adhesion in terms of forces, with the force of adhesion being the maximum force exerted when two adhered materials are separated. Many theories on the mechanisms of adhesion are usually attributed to adsorption, chemical bonding and mechanical interlocking all of which play significant roles in interfacial

Table 1.1 Bonding energy range for different types of bonds [22].

Category	Bond type	Bond energy [kJ/mol]
Primary Bond	Ionic	600–1100
	Covalent	60–700
	Metallic	110–350
	Brönsted acid-base interaction	Up to 1000
Secondary Bond	Hydrogen bonds	Up to 40
	Van der Waals bonds	Up to 40

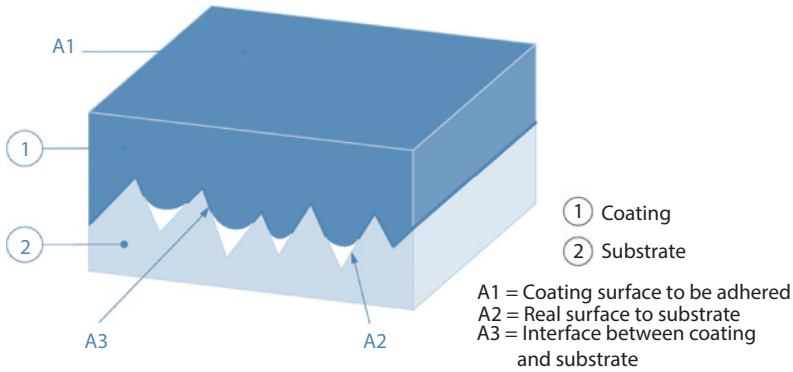

Figure 1.4 Pattern of surface effects determining the overall adhesion [Adapted from [23]].

bonding. The energy required to separate the polymer from a metal surface is a function of the adhesion level i.e. interactions at the interface, but it also depends on the mechanical and viscoelastic properties of the polymeric material.

Modern multi-chip packages have inherent manufacturing variability in chip stacks including IHS flatness, die stack-up gaps and die dynamic warpage affecting TIM_1 and TIM_2 adhesion and BLTs. This, in turn, affects the Rjc (equation 5) and the package reliability. Listed in Table 2 are some of the commercially available TIM_1/TIM_2 materials which exhibit unique adhesion property.

1.2.3 Chemical Bonding

The adhesion results from molecular contact between polymer and substrate due to surface forces. For these forces to develop, the polymer must make an intimate contact with the substrate surface. The process of establishing a continuous contact is termed as wetting which can be measured by contact angle. The prerequisite for wetting is a contact or wetting angle of less than 90 degrees. A complete spontaneous wetting occurs when the contact angle is zero degrees. Schematic illustration of good and poor wetting is presented in

Table 1.2 TIM materials widely used in industry and are commercially viable.

TIM materials	Advantages	Disadvantages
Polymers	1. Conform to surfaces 2. Fail cohesively, depending on polymer chemistry	Physical movement and delamination failure mode
Adhesives	1. Conform to surfaces 2. No physical movement or migration	1. Low thermal conductivity 2. Cure process required 3. Delamination failure mode 4. Not recoverable
Aligned Carbon Fibers	1. Very high thermal conductivity 2. Easy to handle 3. No physical movement or migration	1. High pressure required to compress 2. Not recoverable
Phase-Change Materials	1. High thermal conductivity 2. Compressible 3. Conform to surfaces	1. Difficult to handle 2. Not recoverable
Thermal Greases	1. High thermal conductivity 2. Compressible 3. Conform to surfaces	1. Difficult to handle 2. Not recoverable
Gap Fillers/Gels	1. Conform to surfaces 2. Compressible 3. No physical movement or migration	1. Low thermal conductivity 2. Cure process required 3. Difficult to handle 4. Delamination failure mode 5. Not recoverable
Gap Pads/ Elastomers	1. Easy to handle 2. Fill larger BLT gaps 3. May be recoverable	1. High contact resistance 2. Low thermal conductivity in general

Figure 5. Wetting is favoured when the substrate surface tension (in mN/m), also known as the surface free energy (in mJ/m^2), is higher than that of the adhering polymer. Low surface energy polymers, therefore, easily wet the high surface energy substrates such as metals and glass. On the other hand, substrates with low surface energy such as polyethylene, fluorocarbons, etc. will not be wetted.

Surface tension is an important factor that determines the ability of a polymer coating to wet and adhere to a substrate. The ability of a coating to wet a substrate has been shown to be improved by using solvents with lower surface tensions. Wetting may be quantitatively defined with reference to a liquid drop resting in equilibrium on a solid surface (Figure 5). The smaller the contact angle, the better the wetting. When q is zero, the liquid wets the

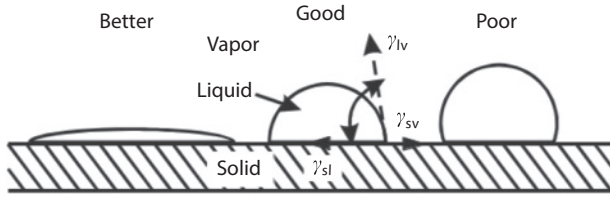

Figure 1.5 Cartoon illustration of good and poor wetting [Adapted from [24]].

solid surface completely at a rate depending on the liquid viscosity and the solid surface roughness. The equilibrium contact angle for a liquid drop sitting on ideally smooth, flat, and nondeformable surface is related to various interfacial tensions by Young's equation:

$$\gamma_{lv} \cos \theta = \gamma_{sv} - \gamma_{sl} \tag{7}$$

Where γ_{lv} is the surface tension of the liquid in equilibrium with its own saturated vapor, γ_{sv} is the surface free energy of the solid in equilibrium with the saturated vapor of the liquid, and γ_{sl} is the interfacial tension between the solid and the liquid. For spontaneous wetting to occur, the surface tension of the liquid must be lower than the surface free energy of the solid. It is also possible for a liquid to spread and wet a solid surface when θ is greater than zero, but this requires the application of a force to the liquid. The ranges of van der Waals forces and the hydrogen bonds are extremely short for this purpose. For optimum adhesion it is, therefore, absolutely essential to ensure good wetting by the coating material applied, thus creating ideal conditions for causing the film forming agent molecules to approach the substrate. The condition for good wetting is always fulfilled whenever the surface free energy of the substrate is higher than that of the liquid coating material. Such a requirement can easily be fulfilled when coating metals because of their high surface free energy. With various nonpolar plastics such as polyethylene or polypropylene, with surface free energy values less than 30 mJ/m^2, it is not possible to achieve good adhering coatings because of the inferior wettability without appropriate surface treatments. The surface tension values of the involved materials, the liquid coating and the solid substrate, are most important for substrate wetting. Figure 6 and Table 3 highlight the surface tension in mN/m or surface free energy in mJ/m^2 of some of the commercially available metals and polymer materials.

It is interesting to note that the polarity of the substrate and possible surface structures (porosity, roughness) will also influence the adhesion mechanism. For example, for surfaces such as wood, the surface tension will not be the same across the whole surface and will vary. Additional surface irregularities can be due to contamination of the surface, which will then cause wetting problems in the form of craters in some areas. Finally, there is also a time aspect. The surface free energy of the substrate is constant, but the surface tension of the liquid phase changes due to solvent evaporation and cross-linking reactions. If, in this process, the surface tension of the liquid exceeds that of the substrate, dewetting can occur, if the film viscosity is still low enough. When a polymeric

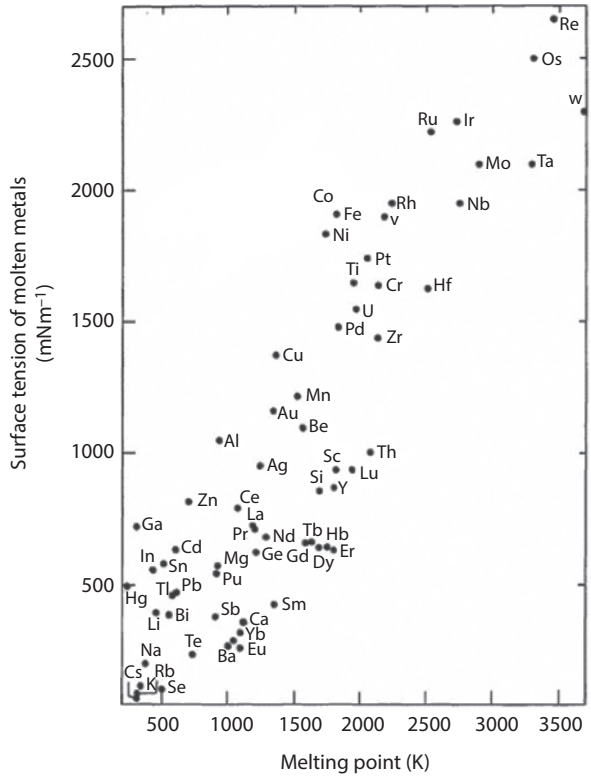

Figure 1.6 Surface tension of molten metals at their melting points [Adapted from [25]].

Table 1.3 Surface tension of commercially available polymers.

Polymer	**Surface tension (mN/m)**
Polyperfluoropropylene	16
Polytetrafluoroethylene (Teflon)	18.5
Poly(dimethylsiloxane)	24
Polyethylene	31
Polystyrene	34
Poly(methyl methacrylate) (acrylic)	39
Poly(vinyl chloride) (PVC)	40
Poly(ethylene terephthalate) (polyester)	43
Poly(hexamethylene adipate) (nylon)	46

coating is applied on a substrate, a chemical reaction takes place between the two materials i.e. the substrate as well as the coating. It is often desirable to modify the substrate to ensure reactivity at the interface by removing contamination and/or introducing functional groups. This simplified view of the interfacial or interphase bonding neglects physical forces between the two materials, which are influenced by surface roughness. For a comprehensive characterisation of coatings, surface analysis of the substrate (chemical as well as topographic) and thermal analysis of cured polymeric coating materials are of great importance.

Due to the higher bonding energy of the primary bonds in comparison to secondary bonds, working on different types of primary bonds has been more attractive for researchers. Various types of primary bonds, such as ionic and covalent at different interfaces have been reported in the literature. For instance, bonding of brass and rubber occurs by curing with the existence of sulfur due to the creation of polysulfide bonds [26]. Using coupling agents, such as adhesion promoter molecules, is one of the most interesting approaches for interfacial chemical bonding. These molecules are able to make a bond with both polymer and metal [27, 28]. The most common adhesion promoters are silane-based molecules. Examples of silane-based adhesion promoters are listed in Table 4.

Schuberth *et al.* [29] used 2,2'-Spirobi[4H-1,3,2-benzodioxasilin] and 2-(3-amino-n-propyl)-2-methyl-4H-1,3,2-benzodioxasilin as twin monomers in order to improve the polymer-metal bonding by introducing chemical bonding between the two. In their work, they considered the interaction of chemical adhesion promoter versus surface treatments on steel-fiber reinforced polymer (FRP) and aluminum-FRP as shown in Figure 7. Interestingly, it was concluded that using these two techniques together was not generally more effective than the individual ones, and surface treatment should be adjusted for the purpose and application.

It is definite that all the mechanisms mentioned above can affect adhesion and thus bond strength. It is also undisputed that the individual mechanisms of adhesion only make significant contributions if the prerequisites have been met. If one endeavors to establish

Table 1.4 Examples of silane-based adhesion promoters reported in the literature.

Adhesion promoter	**Organic structure**
Trimethoxyvinylsilane	$(CH_2)=CHSi(OCH_3)_3$
(3-Chloropropyl)trimethoxysilane	$Cl(CH_2)_3Si(OCH_3)_3$
(3-Mercaptopropyl)trimethoxysilane	$HS(CH_2)_3Si(OCH_3)_3$
(3-Aminopropyl) diethoxymethylsilane	$H_2N(CH_2)_3Si(CH_3)(OC_2H_5)_2$
(3-Aminopropyl) triethoxysilane	$H_2N(CH_2)_3Si(OC_2H_5)_3$
(3-Aminopropyl) trimethoxysilane	$H_2N(CH_2)_3Si(OCH_3)_3$
Triethoxy –(3-ureidopropyl)silane	$H_2NCONH(CH_2)_3Si(OC_2H_5)_3$
Triethoxy –(3-methacryloxypropyl)silane	$CH_2=C(CH_3)COO(CH_2)_3Si(OCH_3)_3$

the causes of interactions, numerous theories are available in the literature [30–33]. The explanations range from mechanical attachment of the coating on the cavities and fissures in the substrate (mechanical anchoring) and attachments of film forming agent molecules by diffusion or contact charges and the creation of mirror forces through interactions of polar functional groups, hydrogen bonds or chemical links between the coating and the substrate as illustrated in Figures 8 and 9. Figure 9 shows curves and ranges of the potential energies of van der Waals forces as well as hydrogen bonds as the causes for adhesion. Van der Waals forces are orientation forces (dipole-dipole), induction forces (dipole/induced dipoles) and dispersion forces. Assuming a suitable chemical structure and an appropriate substrate there are also effective hydrogen bonds.

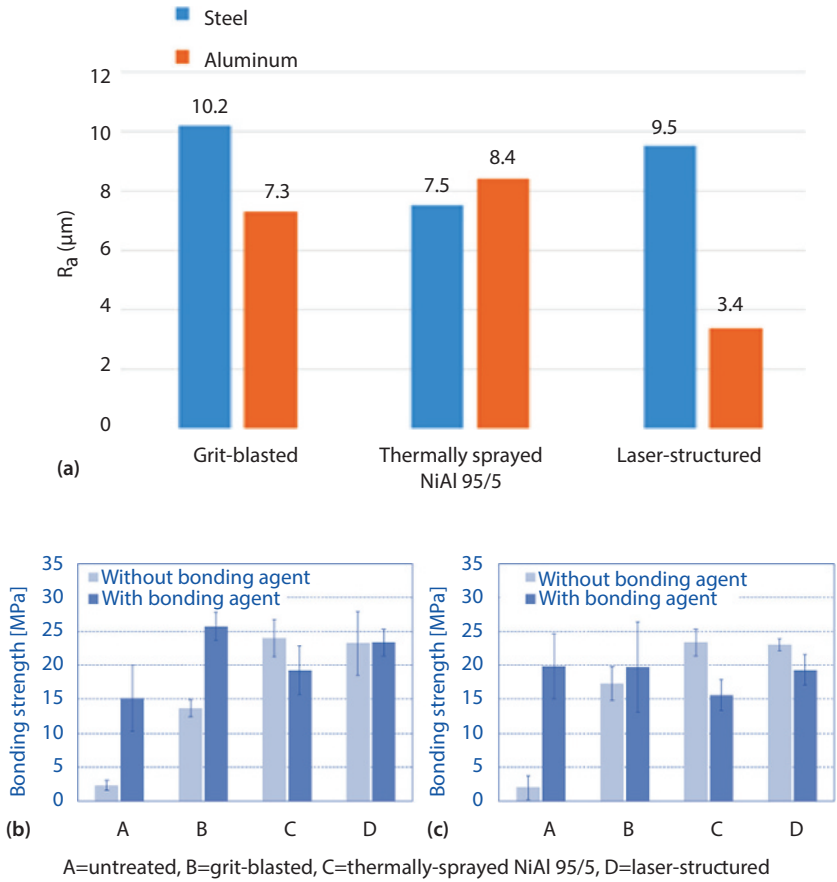

Figure 1.7 (**a**) Surface roughness of steel and aluminum according to different surface treatments. Bonding strength of (**b**) Steel-FRP and (**c**) aluminum-FRP determined by shear tension test [Adapted from [29]].

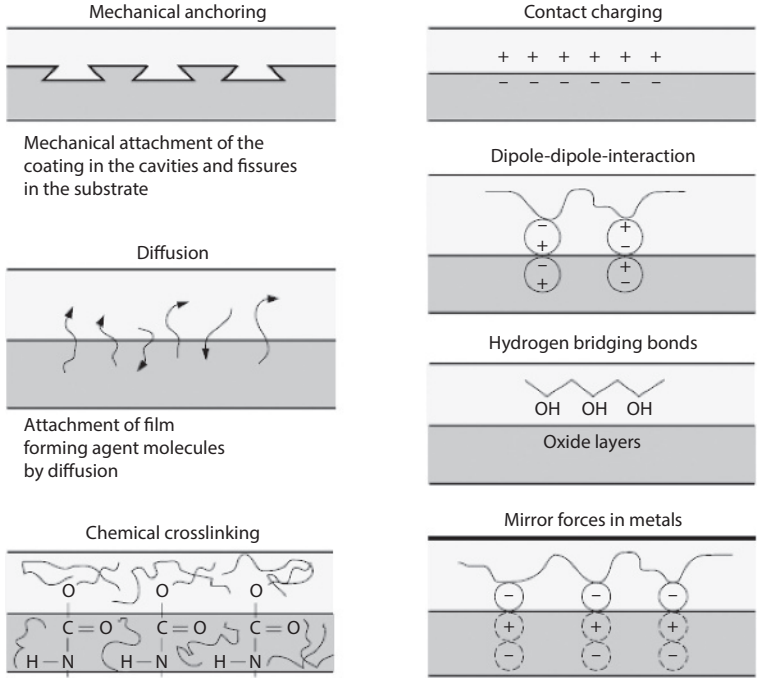

Figure 1.8 Physical and chemical bonding of polymer coatings to the metal surface [Adapted from [23]].

1.2.4 Mechanical Interlocking

Lee and Qu studied the effect of surface roughness by presenting the outcome of different types of oxidation on interfacial fracture toughness [34]. In their study, it was shown that copper as a function of oxidation time from exposure to the environment creates different oxidized forms. Within the first 30 seconds of copper exposure, pebble-like cuprous oxide (Cu_2O) was formed on the surface with an approximate thickness of 0.2 μm. After 2 minutes, needle-shape cupric oxide (CuO) was formed. Formation of cupric oxide causes interfacial (adhesion) failure mechanism in the polymer coating (Figure 10).

Schaubroeck, *et al.* exposed a polymer resin surface to $KMnO_4$/NaOH solution for different time periods to roughen the surface by means of etching [35]. By controlling the time of exposure, surface roughness was controlled and after that surfaces were treated by polydopamine according to the method described by Lee *et al.* [36]. Afterward, copper deposition was carried out on polydopamine (DOPA)-modified and non-modified etched surfaces. Peel strength of the deposited copper on non-modified Epoxy Cresol Novolac (ECN) resin substrates increased by an increment in surface roughness. Moreover, it shows that lower electroplating bath temperature leads to higher peel strength in comparison to higher temperatures as indicated in Figure 11.

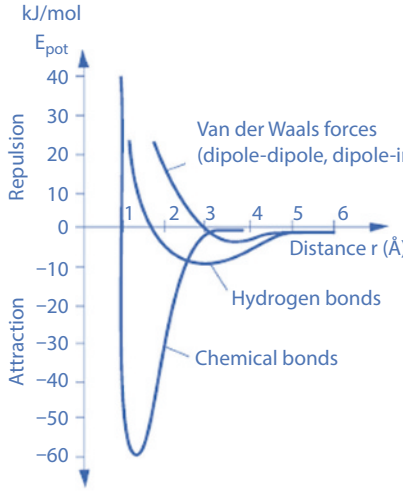

Type of van der Waals forces	Average energy	Range
Orientation forces Dipole-dipole (Keesom forces)	25 kJ/mol	$E= \frac{2\mu^4}{3kTr^6}$
Induction forces Dipole-induced dipole (Debye forces)	15–20 kJ/mol	$E= \frac{2\alpha.\mu^2}{r^6}$
Dispersion forces (London forces)	5–10 kJ/mol	$E= \frac{3hv_0.\alpha}{4r^6}$
Hydrogen bridging bonds	40–50 kJ/mol	$E= e^{-kr}$

Figure 1.9 Potential energies of van der Waals forces as well as hydrogen bonds [Adapted from [23]].

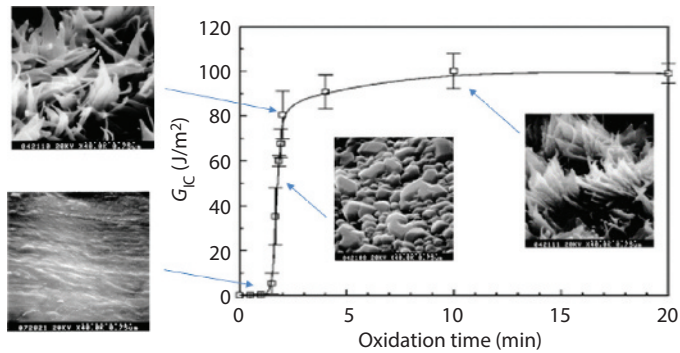

Figure 1.10 Fracture toughness (G_{IC}) as a function of oxidation time and representative SEM images at different times [Adapted from [34]].

On both polydopamine modified substrates as well as non-modified surfaces, peel strength does not have a linear correlation with surface roughness. This result has a striking similarity with Schuberth *et al.* work which showed that employing both adhesion promoter and surface roughness does not necessarily lead to higher bond strength of metal-polymer bonds in comparison to their individual effect [29].

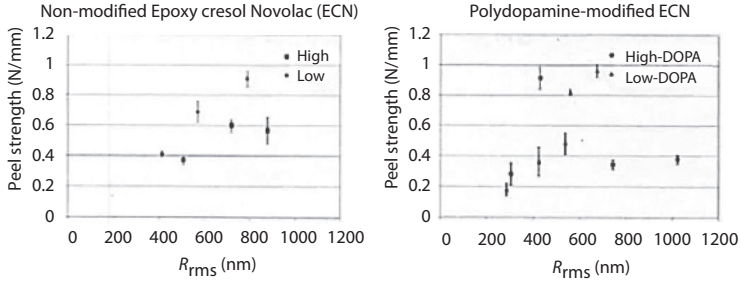

Figure 1.11 Peel strength of the non-modified (left) and polydopamine-(DOPA) modified ECN surface (right) after copper plating on top. Two series of measurements in each graph are representative of low (35°C) and high (47°C) electroless plating temperature [Adapted from [35]].

1.2.5 Weak Boundary Layer

According to a theory proposed by Bikerman, adhesion failures occur due to the presence of a weak layer at the interface between the adhesive and target surface as illustrated in Figure 12 [37]. This theory suggests that the root cause of adhesion failure is the cohesive failure within the weak boundary layer. One of the common weak layers is the hydrocarbon contamination on the target surface [38]. Plasma surface treatment is one of the well-known ways to remove hydrocarbon layer from the surface [39].

Jang *et al.* investigated the nonconductive film (NCF)-SiO_2 adhesion improvement by oxygen plasma cleaning [40]. Applying the oxygen plasma to the oxidized silicon wafer causes removal of the hydrocarbons and increase in silanol groups and hydrophilicity of SiO_2 surface. However, strikingly, surface roughness decreased after plasma treatment in comparison with non-treated surfaces and due to this plasma treatment could not enhance the adhesion despite increment in surface energy. However, de-ionized water (DIW) rinse was applied after surface plasma cleaning. This step could change the surface roughness during plasma treatment due to the presence of hydroxyl groups on the oxidized silicon surface [41, 42]. With DIW rinse step, NCF-SiO_2 bond strength was improved as shown in Figure 13.

In another study, Coulon *et al.* carried out plasma surface treatment on the polymer resin and then covered the surface with 1 μm thick evaporated aluminum film [43]. It was demonstrated regardless of the roughness of the surface, plasma treatment brought about surface energy and adhesion strength increments (Figure 14). X-ray photoelectron spectroscopy (XPS) analysis of treated and non-treated polymer resin surfaces revealed that atmospheric plasma created reactive carbonyl groups and metal-carbonyl bonds led to higher adhesion strength [44, 45].

1.3 Ball Grid Array Solder Attach Adhesion Phenomena

Ball grid array packages have solder balls pre-attached to the bottom of the substrate, hence resulting in a higher stand-off height compared to land grid array packages. This higher

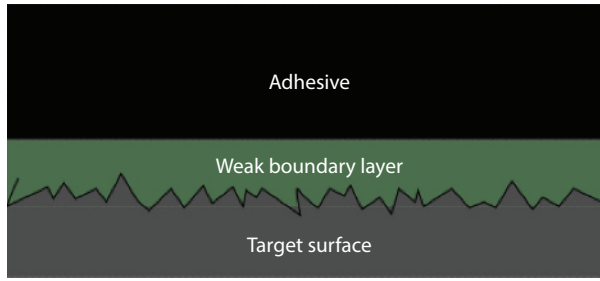

Figure 1.12 Schematic presence of a weak boundary layer, such as environmental contamination, as a failure mechanism in adhesion [Adapted from [37]].

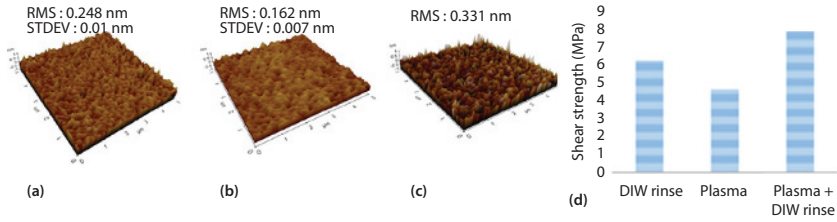

Figure 1.13 Atomic force microscopy (AFM) measurements of surface roughness of (**a**) un-treated (**b**) atmospheric plasma treated (**c**) and surface subjected to both plasma treatment and DIW rinse. (**d**) Shear strength of NCF-SiO_2 bonding with different surface treatments [Adapted from [40]].

stand-off height and improved planarity of the package have been shown to positively affect the temperature cycle performance of the electronic devices [46]. The adhesion/joint quality and reliability of these solder joints and the yields during the surface mount process heavily depend on the material and process selections. The materials involved in the ball attach process are solder sphere, flux, or solder paste. The solder sphere selection determines the strength and reliability of the joint and hence affects its performance under stress and temperature that the devices go through in the field. The flux or solder paste serves to clean the oxide on the solder sphere and the pad on the substrate and attaches the solder sphere through a metallurgical joint.

1.3.1 Solder Alloy Selection

Tin-silver-copper alloys are widely used as a lead-free alternative in the semiconductor packaging industry. This is because they possess an attractive combination of wettability to the pad surface, good mechanical properties, microstructural stability and availability [47]. However, the melting range of tin-silver-copper (SnAgCu, also known as SAC) alloys is

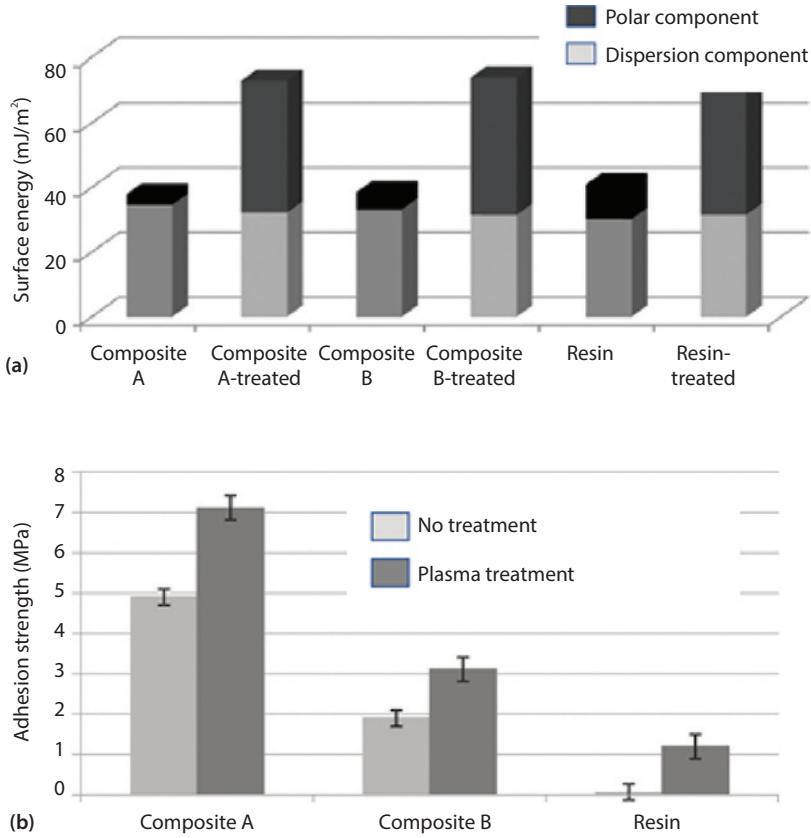

Figure 1.14 (**a**) Surface energy evolutions on different surfaces before and after atmospheric plasma treatment, (**b**) adhesion strength of physical vapor deposited Al on top of the un-treated and plasma treated composites and resin [Adapted from [43]].

high and requires a typical reflow peak temperature of 245 °C. This leads to higher warpage of the package during assembly and may lead to poor joint formation or adhesion [48]. Since Sn is a reactive species, the same intermetallic compounds are formed with both Cu and Ni surfaces during solder/substrate interaction between all common Sn-based solders such as Sn-Ag-Cu, Sn-Cu, and Sn-Bi alloys [49]. With a Cu surface, these alloys form Cu_3Sn and Cu_6Sn_5 as can be seen in the phase diagram that these two are the stable intermetallic compositions in the temperature range of interest [50]. With a Ni surface, these alloys primarily form Ni_3Sn_4 and it can be seen that this is one of the stable compositions in the phase diagram and forms at the lowest temperature upon cooling among all intermetallics [51]. When Cu is present in the solder, even in much lower amount than Sn, $(Cu, Ni)_6 Sn_5$ intermetallic is observed as well.

Once the joint is formed, it is important that the adhesion holds or the joint survives through mechanical shock and severe thermal changes due to operation of the device as well as external changes in temperature [52]. Under mechanical shock, the primary mode of failure is cracking along the intermetallic layer as seen in Figure 15.This is primarily because at high strain rates, the yield strength of the bulk solder increases drastically making the intermetallic layer the weaker portion of the joint [53]. This is referred to as strain-rate sensitivity. It has been found that a decrease in elastic modulus, which is modulated primarily by the composition of the solder, and a decrease in yield strength can help in increasing the overall toughness of the joint during shock, for example SAC105 showed better shock resistance than SAC405 [54]. A lower silver content was found to be generally associated with higher ductility and lower strength of SAC solders in the 0-5% range [55]. The other method to improve shock resistance would be to change the nature and properties of the intermetallic layer itself. This has been achieved by addition of Ni to SAC alloys for example [52]. The effect of Ni addition, in the right proportion, was found to decrease intermetallic thickness or growth through void reduction and also through increasing the liquidus temperature of the solder [56, 57].

Under thermal cycling, however, the crack originates and propagates through the body of the solder [52]. The crack nucleation sites include the interfaces between the intermetallics and the bulk solder and the grain boundaries of the bulk solder created by localized recrystallization reactions due to differential plastic strain stored within the solder [59]. The crack growth has been proposed to be an intergranular propagation along the recrystallized network of high angle grain boundaries as illustrated in Figure 16 [59, 60]. Due to the dependence of recrystallization on the critical strain energy, higher strength alloys were shown to be beneficial, however, this could also result in poor drop shock performance as discussed earlier.

Sn-Bi solders are lower melting alternatives to SAC solders. It was found that Sn-Bi solders wetted Au/Ni/Cu surface better than bare Cu or bare Ni [61]. In addition, the

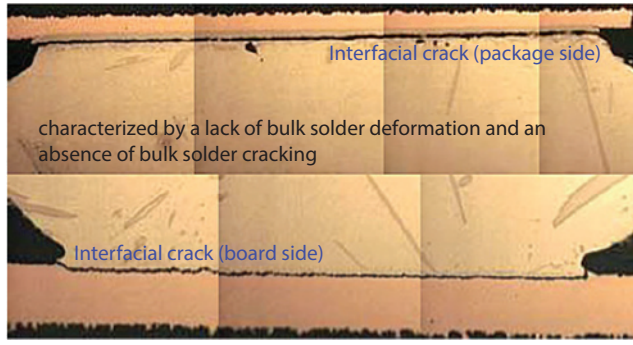

Figure 1.15 An example of a typical failure mode of solder joint (SAC 405) under mechanical shock or high strain rate deformation [Adapted from [58]].

interfacial tension between the liquid solder and substrate decreases with an increase in Bi content leading to better wetting at higher Bi concentrations [61]. The relationship between wettability, surface energy and adhesion/joint strength has been discussed [62]. One study found that a Sn-30Bi-0.5Cu alloy had a much lower contact angle or superior wettability to an SAC305 solder [63]. However, a composition beyond the eutectic concentration of Bi (58%) leads to embrittlement due to the presence of Bi-rich phase [64]. In addition, once the Sn is depleted for intermetallic compound formation, a Bi-rich layer forms adjacent to the interface leading to potential weakness in the solder joint [65].

1.3.2 Flux Selection

Flux type, composition and quantity play a crucial role in controlling the adhesion of the solder to the pad. In addition, they also might modulate the adhesion of other materials such as the underfill (though not directly relevant to second-level interface), when a no-clean flux is used [66]. Fluxes used for soldering in the microelectronics industry including the ball attach process fall into two major categories: no-clean and water washable. No-clean fluxes do leave a residue while any water washable flux can be removed by washing with water, which is typically heated and sprayed. However, no-clean flux residues are hydrophobic in nature and cannot be water washed but these are tolerated since they are nonconductive and noncorrosive [67, 68]. The flux reactions with the substrate pad and the solder sphere are much more than just oxidation-reduction and involve acid-base, co-ordination and adsorption type reactions as well. Most fluxes form salt and water with metallic oxides and the salt further helps in promoting solder wetting [69].

In general, for proper adhesion, fluxing of lead-free solders such as SAC alloys is more challenging than lead containing solders. This has been attributed to 3 different factors: 1.

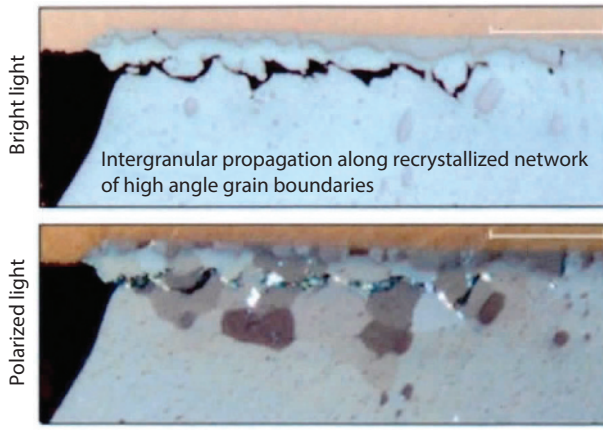

Figure 1.16 Intergranular crack propagation during thermal cycling of an SAC alloy [Adapted from [60]].

Tin salt that forms at high temperatures is harder to clean than lead salt, 2. Higher flux activity is needed to boost the wetting of an SAC solder leading to more side reactions, and 3. Higher reflow profile is needed for SAC compared to an eutectic Sn-Pb solder. There are other challenges caused by lead-free solder alloys other than SAC alloys, prevalent in the industry today. Low temperature solders such as Sn-Bi need fluxes with a lower activation temperature and highly oxidizable alloys such as the ones containing Zn need a flux with a high oxygen barrier capability or needs to be reflowed under an inert atmosphere [67]. Hence modern fluxes need to have a superior compatibility to lead-free solders based on factors such as superior thermal stability, etching ability, and a temperature range of activity that is compatible with the melting range of the solder. This often necessitates custom development based on solder alloy package/board pad surface finish selection.

1.4 Summary

In this review paper, a detailed overview of interfacial adhesion phenomena of the polymer layers to a metal surface is given. Various bonding mechanisms which play a key role in polymer to metal bonding are discussed in detail. For optimum adhesion, it is absolutely essential to ensure good wetting. Ideally, for good substrate wetting the surface tension of the polymer material should be lower than the surface tension of the substrate. The quality and durability of polymer to metal bonding are directly related to the nature of adhesion. Many theories influencing the mechanism of interfacial adhesion including adsorption, chemical bonding and mechanical interlocking are discussed. The energy required to separate the polymer from a metal surface also depends on the properties of the polymer material. It is definite that all the mechanisms mentioned could modulate the adhesion and thus the bond strength.

Novel ideas and procedures to enhance polymer to metal bonding and to mitigate adhesion failures are provided which include chemical surface modification and plasma treatment. According to Schuberth *et al.* [29] and Schaubroeck *et al.* [35] surface chemical modification and adhesion promoters used in combination on the metallic surface do not necessarily enhance the bond strength significantly compared to employing them individually on the surface. In other words, efficacy of adhesion promoters depends on the surface and it is more effective on smoother surfaces. In another section, the effect of plasma treatments of polymer substrates is reviewed. Jang *et al.* [40] studied the adhesion phenomena of SiO_2 substrates using oxygen plasma treatment with and without de-ionized water treatment. Coulon *et al.* [43] measured the adhesion strengths on carbon/epoxy composite surfaces treated with atmospheric plasma. Remarkably, from these two works, it becomes clear that there is a difference in applying plasma treatment on oxidized silicon surfaces as opposed to polymer surfaces. In Jang *et al.* work [40], it was shown that plasma treatment on SiO_2 showed no enhancement in its surface roughness and did not add any value to bond strength. Use of de-ionized water after plasma treatment helped to improve bond strength drastically with the formation of $Si(OH)_x$ bonds. But on the other hand, Coulon *et al.* [43] demonstrated that plasma treatment of the polymer surface, regardless of its roughness, would help PVD coated aluminum bond strength.

To assemble latest technology BGA microelectronic packages with improved reliability and performance has been one of the challenging tasks for semiconductor industries. It involves mounting solder balls onto the land side of the substrate. The adhesion and survivability of solders depend heavily on selection of solder spheres and flux materials. The melting range of the solders has a significant effect on package warpage and its bonding phenomena. Sn-Ag-Cu or SAC solders are the common choice for lead-free solder spheres and it has been found that an increase in the silver content leads to superior thermal cycling survivability but poor shock survivability and vice versa. Bi tends to increase the strength of the solder and Bi containing low melting solder is available, however, it can lead to embrittlement of the joint. Fluxes fall into no-clean and water washable categories and selection needs to be made here based on application and tolerability. Fluxing SAC solders is much more challenging when compared to lead based solders for several reasons and the flux choice needs to be made suitably as well with regards to activation range, thermal stability and oxide-removal capability.

Nomenclature

A_{die}	Area of a Semiconductor Chip
BGA	Ball Grid Array
BLT	Bond Line Thickness
Cu_2O	Cuprous Oxide
CuO	Cupric Oxide
DIW	De-ionized Water
ECN	Epoxy Cresol Novolac
FRP	Fiber Reinforced Polymer
IHS	Integrated Heat Spreader
k_{TIM}	Thermal Conductivity of the Thermal Interface Material
LGA	Land Grid Array
NCF	Non-Conductive Film
PCB	Printed Circuit Board
PTIM	Polymer Thermal Interface Material
R_{c1}	Contact Resistance of the TIM at the Silicon to TIM Interface
R_{c2}	Contact Resistance of the TIM at the TIM to Metal Interface
R_{jc}	Thermal Impedance at the Junction to IHS Surface
SMT	Surface Mount Technology
STIM	Solder Thermal Interface Material
TIM	Thermal Interface Material
TIM_1	Die to IHS Thermal Interface Material Layer
TIM_2	IHS to Heat Sink Thermal Interface Material Layer
T_a	Ambient Air Temperature
TDP	Thermal Design Power
T_c	Integrated Heat Spreader Temperature

T_j Maximum Junction Temperature
T_{sink} Heat Sink Temperature
XPS X-ray Photoelectron Spectroscopy
Ψ_{ja} Overall Thermal Resistance
Ψ_{jc} Package Thermal Resistance
Ψ_{ca} System Thermal Resistance

References

1. S. J. Dent, L. J. Larson, R. T. Nelson, and D. C. Rash, Semiconductor package and method of preparing the same, US Patent 6940177 (2005).
2. S. F. De Cecco and G. W. Cheshire, Cooling assembly using Heat Spreader, US Patent 9318410 (2016).
3. A. B. Chong, Multi-chip packaging (MCP) or not MCP, in Proc. of the International MultiConference of Engineers and Computer Scientists (IMECS), Vol. II, pp. 1–4 (2012).
4. R. Mahajan, C. P. Chiu, and G. Chrysler, Cooling a microprocessor chip. *Proc. IEEE* 94, 1476–1486 (2006).
5. L. A. Polka, H. Kalyanam, G. Hu, and S. Krishnamoorthy, Package technology to address the memory bandwidth challenge for Tera-scale computing. *Intel Technol. J.* 11, 197–205 (2007).
6. I. Sauciuc, R. Prasher, J. Y. Chang, H. Erturk, G. Chrysler, C. P. Chiu, and R. Mahajan, Thermal performance and key challenges for future CPU cooling technologies, in Proceedings of IPACK2005, ASME InterPACK'05, San Francisco, California, USA (2005).
7. R. Mahajan, C.P. Chiu, and R. Prasher, Thermal interface materials: A brief review of design characteristics and materials, *Electronics Cooling* 10, 1–12 (2004).
8. R. Prasher, Thermal interface materials: Historical perspective, status, and future directions. *Proc. IEEE* 94, 1571–1586 (2006).
9. K. L. Mittal and T. Ahsan (Eds.), *Adhesion in Microelectronics*, Wiley-Scrivener, Beverly, MA (2014).
10. H. K. Dhavaleswarapu, C. M. Jha, S. F. Smith, S. Kothari, B. Bicen, S. K. Saha, and A. Gupta, Challenges and opportunities in thermal management of multi-chip packages, in *Proc. InterPACK*, Vol. 1, pp. 1–7 (2015).
11. R. D. Lowe Jr, S. Jain, and J. C. Matayabas, Polymer thermal interface material having enhanced thermal conductivity, US Patent Application 20140264818 (2014).
12. B. Liu, S. Jain, J. C. Viskota, N. R. Raravikar, and J. C. Matayabas, Adhesive polymer thermal interface material with sintered fillers for thermal conductivity in micro-electronic packaging, US Patent Application 2017111945 (2017).
13. A. N. Gent and G. R. Hamed, Fundamentals of adhesion, in *Handbook of Adhesives*, 3rd ed., I. Skeist (Ed.), pp. 39–73, Springer US, New York (1990).
14. J. Schultz and M. Nardin, Theories and mechanisms of adhesion, in *Handbook of Adhesive Technology*, A. Pizzi and K. L. Mittal (Eds.), pp. 19–33, Marcel Dekker, New York (1994).
15. D. E. Packham, The mechanical theory of adhesion, in *Handbook of Adhesive Technology*, 2nd ed., A. Pizzi and K. L. Mittal (Eds.), pp. 69–93, CRC Press, Boca Raton, FL (2003).
16. D. J. Gardner, Theories or mechanisms of adhesion, in *Handbook of Adhesive Technology*, 3rd ed., A. Pizzi and K. L. Mittal (Eds.), pp. 3–18, CRC Press, Boca Raton, FL (2018).

17. J. W. McBain and D. G. Hopkins, On adhesives and adhesive action. *J. Phys. Chem*. 29, 188–204 (1925).
18. J. D. Venables, Adhesion and durability of metal-polymer bonds. *J. Mater. Sci*. 19, 2431–2453 (1984).
19. M. M. Chehimi, A. Azioune, and E. Cabet-Deliry, Acid-base interactions: Relevance to adhesion and adhesive bonding, in *Handbook of Adhesive Technology*, 2nd ed., A. Pizzi and K. L. Mittal (Eds.), pp. 95–144, CRC Press, Boca Raton, FL (2003).
20. F. M. Fowkes, Acid-base interactions in polymer adhesion, in *Physicochemical Aspects of Polymer Surfaces*, Vol. 2, K. L. Mittal (Ed.), pp. 583–603, Plenum Press, New York (1983).
21. K. L. Mittal (Ed.), *Acid-Base Interactions: Relevance to Adhesion Science and Technology*, Vol. 2, CRC Press, Boca Raton, FL (2000).
22. L. Pauling, *The Nature of the Chemical Bond and the Structure of Molecules and Crystals*: *An Introduction to Modern Structural Chemistry*, 3rd ed., Cornell University Press, Ithaca, NY (1960).
23. A. Goldschmidt and H. J. Streitberger, Coatings, in *BASF Handbook on Basics of Coating Technology*, W. Andrew (Ed.), pp. 323–433 (2003).
24. A. C. Santos, A. P. Luz, and S. Ribeiro, Melting temperature and wetting angle of AlN/Dy_2O_3 and AlN/Yb_2O_3 mixtures on SiC substrates. *J. Mater. Res*. 18, 957–962 (2015).
25. B. J. Keene, Review of data for the surface tension of pure metals. *Intl. Mater. Reviews* 38, 157–192 (1993).
26. H. Neusser and W. Schall, Studies on some promising possibilities for improvement of plywood. 1. Gluing with aminoplasts, *Holzforschung Holzverwertung* 24, 108–116 (1972).
27. M. Huang and E. R. Pohl, Organofunctional silanes for sealants, in *Handbook of Sealant Technology*, K. L. Mittal and A. Pizzi (Eds.), pp. 27–49, CRC Press, Boca Raton, FL (2009).
28. K. L. Mittal (Ed.), *Silanes and Other Coupling Agents*, Vol. 4, CRC Press, Boca Raton, FL (2007).
29. A. Schuberth, M. Goring, T. Lindner, G. Toberling, M. Puschmann, F. Riedel, I. Scharf, K. Schreiter, S. Spange, and T. Lampke, Effect of new adhesion promoter and mechanical interlocking on bonding strength in metal-polymer composites, *IOP Conf. Ser. Mater. Sci. Eng*. 118, 1–6 (2016).
30. C. Bischof and W. Possart, *Adhäsion: Theoretische and Experimentelle Grundlagen*, Akademie-Verlag (1983).
31. J. Comyn, Theories of adhesion, in *Handbook of Adhesives and Sealants*, P. Cognard (Ed.), Vol. 2, pp. 1–50, Elsevier (2006).
32. W. C. Wake, Theories of adhesion and uses of adhesives: A review, *Polymer* 19, 291–308 (1978).
33. D. E. Packham, The mechanical theory of adhesion- changing perceptions 1925–1991. *J. Adhesion* 39, 137–144 (1992).
34. H. Y. Lee and J. Qu, Microstructure, adhesion strength and failure path at a polymer/roughened metal interface. *J. Adhesion Sci. Technol*. 17, 195–215 (2003).
35. D. Schaubroeck, E. Van Den Eeckhout, J. De Baets, P. Dubruel, L. Van Vaeck, and A. Van Calster, Surface modification of a photo-definable epoxy resin with polydopamine to improve adhesion with electroless deposited copper. *J. Adhesion Sci. Technol.* 26, 2301–2314 (2012).
36. H. Lee, S. M. Dellatore, W. M. Miller, and P. B. Messersmith, Mussel-inspired surface chemistry for multifunctional coatings. *Science* 318, 426–430 (2007).
37. J. J. Bikerman, Causes of poor adhesion: Weak boundary layers. *Ind. Eng. Chem*. 59, 41–44 (1967).
38. W. C. Luo, Surface property of passivation layer on integrated circuit chip and solder mask layer on printed circuit board, IEEE Trans. Electron. *Packag. Manuf*. 26, 345–351 (2003).
39. D. F. O'Kane and K. L. Mittal, Plasma cleaning of metal surfaces. *J. Vac, Sci. Technol*. 11, 567–569 (1974).

40. M. S. Jang, S. W. Ma, J. Song, M. Sung, and Y. H. Kim, Adhesion of NCF to oxidized Si wafers after oxygen plasma treatment, *Microelectron. Reliab*. 78, 220–226 (2017).
41. A. U. Alam, M. M. R. Howlader, and M. J. Deen, Oxygen plasma and humidity dependent surface analysis of silicon, silicon dioxide and glass for direct wafer bonding. *ECS J. Solid State Sci. Technol*. 2, 515–523 (2013).
42. S. Bengtsson and P. Amirfeiz, Room temperature wafer bonding of silicon, oxidized silicon, and crystalline quartz. *J. Electronic Mater*. 29, 909–915 (2000).
43. J. F. Coulon, N. Tournerie, and H. Maillard, Adhesion enhancement of Al coatings on carbon/epoxy composite surfaces by atmospheric plasma. *Appl. Surf. Sci.* 283, 843–850 (2013).
44. M. Thomas and K. L. Mittal (Eds.), *Atmospheric Pressure Plasma Treatment of Polymers*, Wiley-Scrivener, Beverly, MA (2013).
45. M. Strobel, C. S. Lyons, and K. L. Mittal (Eds.), *Plasma Surface Modification of Polymers: Relevance to Adhesion*, CRC Press, Boca Raton, FL (1994).
46. S. Joshi, B. Arfaei, A. Singh, M. Gharaibeh, M. Obaidat, A. Alazzam, M. Meilunas, L. Yin, M. Anselm, and P. Borgesen, LGAs vs. BGAs-lower profile and better reliability, in Proc. Surface Mount Technology Association International Conference, pp. 1–4 (2012).
47. Y.T. Chin, P.K. Lam, H.K. Yow, and T.Y. You, Investigation of mechanical shock testing of lead-free SAC solder joints in fine pitch BGA package. *Microelectron. Reliab*. 48, 1079–1086 (2008).
48. L. Kondrachova, S. Aravamudhan, R. Sidhu, and D. Amir, Fundamentals of the non-wet open BGA solder joint defect formation, in Proc. International Conference on Soldering and Reliability (ICSR), pp. 1–4 (2012).
49. J. Glazer, Microstructure and mechanical properties of Pb-free solder alloys for low-cost electronic assembly: A review. *J. Electronic Mater*. 23, 693–700 (1994).
50. J.H. Shim, C.S. Oh, B.J. Lee, and D.N. Lee, Thermodynamic assesment of the Cu-Sn system. *Zeitschrift Metallkunde*. 87, 205–212 (1996).
51. P. Møller, J.B. Rasmussen, S. Kohler, and L.P. Nielsen, Electroplated Tin-Nickel coatings as a replacement for Nickel to eliminate Nickel dermatitis. National Association for Surface Finishing (NASF) Surface Technology White Papers 78, 15–24 (2013).
52. T. T. Mattila, J. Hokka, and M. Paulasto-Krockel, The reliability of microalloyed Sn-Ag-Cu solder interconnections under cyclic thermal and mechanical shock loading. *J. Electronic Mater.* 43, 4090–4102 (2014).
53. J. H. L. Pang and F. X. Che, Drop impact analysis of Sn–Ag–Cu solder joints using dynamic high-strain rate plastic strain as the impact damage driving force, in Proc 56th IEEE-ECTC Conf, pp. 49–54 (2006).
54. D. Suh, Dong W. Kim, P. Liu, H. Kim, K. A. Weninger, C. M. Kumar, A. Prasad, B. W. Grimsley, and H. B. Tejada, Effects of Ag content on fracture resistance of Sn-Ag-Cu lead-free solders under high-strain rate conditions. *Mater. Sci. Eng: A*., 460, 595–603 (2007).
55. J. Keller, D. Baither, U. Wilke, and G. Schmitz, Mechanical properties of Pb-free SnAg solder joints. *Acta Materialia* 59, 2731–2741 (2011).
56. L. Garner, S. Sane, D. Suh, T. Byrne, A. Dani, T. Martin, M. Mello, M. Patel, and R. Williams, Finding solutions to the challenges on package interconnect reliability, *Intel Technol. J.* 9, 297–308 (2005).
57. V. Vuorinen, T. Laurila, T. Mattila, E. Heikinheimo, and J.K. Kivilahti, Solid state reactions between Cu(Ni) alloys and Sn. *J. Electronic Mater*. 36, 1355–1362 (2007).
58. D. A. Shnawah, M. F. M. Sabri, and I. A. Badruddin, A review on thermal cycling and drop impact reliability of SAC solder joint in portable electronic products. *Microelectron. Reliab*. 52, 90–99 (2012).

59. D. Schmitz, S. Shirazi, L. Wentlent, S. Hamasha, L. Yin, A. Qasaimeh, and P. Borgesen, Towards a quantitative mechanistic understanding of the thermal cycling of SnAgCu solder joints, in Proc. Electronic Components and Technology Conference, pp. 371–378 (2014).
60. H. Chen, M. Mueller, T.T. Mattila, J. Li, X. Liu, K-J Wolter, and M Paulasto-Krockel, Localized recrystallization and cracking of lead-free solder interconnections under thermal cycling. *J. Mater. Res*. 26, 2103–2116 (2011).
61. C. Lee, S. Jung, Y. Shin, and C. Shur, The effect of Bi concentration on wettability of Cu substrate by Sn-Bi solders. *Mater. Trans*. 42, 751–755 (2001).
62. K. L. Mittal, The role of the interface in adhesion phenomena. *Polym. Eng. Sci*. 17, 467–473 (1977).
63. X. Zhang, H. Matsuura, F. Tsukihashi, and Z. Yuan, Wettability of Sn-Zn, Sn-Ag-Cu and Sn-Bi-Cu alloys on copper substrates. *Mater. Trans*. 53, 926–931 (2012).
64. M. McCormack, H.S. Chen, G.W. Kammlott, and S. Jin, Significantly improved mechanical properties of Bi-Sn solder alloy by Ag-doping. *J. Electronic Mater*. 26, 954–958 (1997).
65. L. E. Felton, C. H. Raeder, and D. B. Knorr, The properties of Tin-Bismuth alloy solders. *J. Metals* 45, 28–32 (1993).
66. S. K. Tran, D. L. Questad, and B. G. Sammakia, Adhesion issues in flip-chip on organic modules, IEEE Trans. *Components Packaging Technol*. 22, 519–524 (1999).
67. N. C. Lee and M. Bixenman, Flux technology for lead-free alloys and its impact on cleaning, in Proc. Electronic Components and Technology Conference, pp. 316–322 (2002).
68. C. L Chung, K. S Moon, and C. P. Wong, Influence of flux on wetting behavior of lead-free solder balls during the infrared-reflow process. *J. Electronic Mater*. 34, 994–1001 (2005).
69. G. J. Sprokel, The use of radioisotopes to determine the chemistry of solder flux. *IBM J. Res. Development* 5, 218–225 (1961).